YALE PEABODY MUSEUM

JOURNAL OF MARINE RESEARCH

The *Journal of Marine Research,* one of the oldest journals in American marine science, published important peer-reviewed original research on a broad array of topics in physical, biological, and chemical oceanography vital to the academic oceanographic community in the long and rich tradition of the Sears Foundation for Marine Research at Yale University.

An archive of all issues from 1937 to 2021 (Volume 1–79) are available through EliScholar, a digital platform for scholarly publishing provided by Yale University Library at https://elischolar.library.yale.edu/.

Requests for permission to clear rights for use of this content should be directed to the authors, their estates, or other representatives. The *Journal of Marine Research* has no contact information beyond the affiliations listed in the published articles. We ask that you provide attribution to the *Journal of Marine Research.*

Yale University provides access to these materials for educational and research purposes only. Copyright or other proprietary rights to content contained in this document may be held by individuals or entities other than, or in addition to, Yale University. You are solely responsible for determining the ownership of the copyright, and for obtaining permission for your intended use. Yale University makes no warranty that your distribution, reproduction, or other use of these materials will not infringe the rights of third parties.

Modeling eddy transport of passive tracers

by Russ E. Davis[1]

ABSTRACT

The mean advective and eddy transport of a passive scalar property is examined. Using a theory based on rational approximation of Lagrangian particle statistics, a transport equation relating the mean eddy flux and the mean concentration field Θ is developed. The transport equation is an elaborated advection-diffusion model in which the mean eddy flux is determined by the recent history of the gradient of Θ. The flux law involves an eddy diffusivity which depends on time lag and is defined in terms of fluid particle trajectories. Particle trajectories in simulated geophysical turbulence are used to test the applicability of the restrictions upon which the model is based. Examples are given of how Θ fields are affected by the difference between an advection-diffusion model and its elaborated relative.

1. Introduction

The challenge of ocean dynamics is not only its subtlety but also its complexity in terms of the number of degrees-of-freedom required to describe it deterministically. To cope with this, the effects of small-scale processes on larger scales are frequently parameterized in terms of the large-scale field. In this the "eddy diffusion" analogy with molecular transport has become conventional if not venerable. This analogy has been justified by fundamentally phenomenological "mixing-length" arguments. It has also been justified on somewhat more fundamental grounds using the assumption that the transport process is Markovian and that the dispersing eddies are small compared with the scales of the mean field. The purpose of this paper is to examine the development of related transport models for the simplest case of a passive scalar quantity (passive in the sense that it does not dynamically affect the velocity field).

Of concern are scalar fields θ obeying

$$\partial_t\theta + \mathbf{u} \cdot \nabla\theta = q \tag{1.1}$$

where $\mathbf{u}$ the nondivergent continuum velocity field and q is the source of θ, including the convergence of molecular fluxes. Interest is focused on the mean concentration of Θ defined by the average $\langle \cdot \rangle$. Formally this average is an ensemble mean over many examples of Θ evolution from identically prepared initial and source fields. Motivated by problems like analysis of the quasi-steady general circulation, it is assumed that

statistics of the flow field are stationary so that when applied to flow properties $\langle \cdot \rangle$ can be a time average. The challenge here is to model the effects of fluctuations on evolution of the mean field. The conventional framework for this involves the separation $\Theta = \langle \theta \rangle$, $\theta' = \theta - \Theta$, $\mathbf{U} = \langle \mathbf{u} \rangle$ and $\mathbf{u}' = \mathbf{u} - \mathbf{U}$ in terms of which Θ evolves as

$$\partial_t \Theta + \mathbf{U} \cdot \nabla \Theta = Q - \nabla \cdot \mathbf{E} \tag{1.2}$$

where

$$Q(\mathbf{x}, t) = \langle q(\mathbf{x}, t) \rangle, \qquad \mathbf{E}(\mathbf{x}, t) = \langle \mathbf{u}'(\mathbf{x}, t) \theta'(\mathbf{x}, t) \rangle.$$

$\mathbf{E}$ is the mean eddy flux of Θ-stuff and is what must be related to mean properties.

The phenomenological approach to parameterizing the eddy flux is simply to assert an anlogy between eddies and molecules and invoke a flux *vs.* mean gradient law. This analogy must be questioned unless there is a large separation of time and space scales between fluctuations and the mean fields, as there is in the molecular case. A somewhat more satisfactory approach (*cf.* Csanady, 1973) is based on the assumption that, over some time step, particle motion is a Markov process in the sense that a particle's displacement over the time step does not depend on the particle's history. As shown in the Appendix, the Markov assumption coupled with the restriction that the mean field's scale is much larger than the distance a particle travels over the time step can be used to develop an advection-diffusion equation. As discussed in the Appendix, the weaknesses of this development are (i) the minimum useable Markov time step is difficult to determine when the flow is statistically inhomogenous, as it is in the presence of mean shear or confining boundaries, (ii) the "eddy diffusivity" depends strongly on the mean flow and on the time step, and (iii) the scale separation restriction is severe even for optimistic estimates of the minimum time step.

For these reasons it would be desirable to develop a transport equation by rational approximation. The approach examined here is to average the formal solution to the Lagrangian form of (1.1),

$$\frac{d\theta}{dt} = q, \tag{1.3}$$

rather than to work with the averaged equation (1.2). This provides a specification for the mean field in terms of the mean source Q and the statistics of the Lagrangian trajectories along which (1.3) pertains. The important point is that mean field evolution is fully determined by the mean initial and source fields and the statistics of single Lagrangian particles. While multi-particle statistics are required to describe the relative dispersion of particles making up individual property clouds (the dispersion producing the stirring that leads to mixing), the mean field is fully determined by single-particle statistics.

Because the approach here is based on solving (1.3) before it is averaged, no empirical parameters are introduced and the fluid's transport capacity is specified in terms of particle statistics which are, in principle, observable. Rational approximation of the averaged solution leads to an evolution equation for the mean field. This equation involves advection by the Eulerian mean velocity $U(x)$ and eddy dispersion which is characterized by a time-dependent eddy diffusivity defined in terms of Lagrangian particle statistics. The new transport equation is an elaborated advection-diffusion model in which the elaboration accounts for the finite scales of the dispersing eddies. Under specific conditions, which can be identified from observations of the eddy diffusivity, the transport model reduces to the familiar advection-diffusion equation.

The transport equation, developed in Section 2, rests on certain restrictions on the flow field. In Section 3 analysis of particle motion in simulated geophysical turbulence is used to test the applicability of these restrictions. These simulations also show how mean transport is influenced by physical effects such as variation of the Coriolis parameter, mean shear and confining boundaries. In Section 4 some of the implications of the transport equation, and its relation to a pure advection-diffusion model, are discussed.

2. The transport model

The purpose of this section is to develop a transport model through rational approximation of the exact solution to (1.3). The development is simple once the notation for averaging is understood. Quantities referenced to the Eulerian coordinates position and time are denoted by a parameter list without a vertical bar; thus $u(x, t)$ is the velocity at x, t. The average of such quantities, for example $U(x) = \langle u(x, t) \rangle$, is the Eulerian time average at location x. Primed quantities are always departures from the Eulerian mean. Quantities, such as velocity or position, referenced to particles contain a vertical bar in the parameter list and the variables following the bar are the Lagrangian labels of the particle. For example, $r(t|\tilde{x}, \tilde{t})$ is the position at time t of the particle passing through $\tilde{x}, \tilde{t}$. The velocity of a particle is $u(t|\tilde{x}, \tilde{t})$ where

$$\partial_t r(t|\tilde{x}, \tilde{t}) = u(t|\tilde{x}, \tilde{t}) = u\{r(t|\tilde{x}, \tilde{t}), t\}, \qquad r(\tilde{t}|\tilde{x}, \tilde{t}) = \tilde{x}. \tag{2.1}$$

A particle can be labelled by any $\tilde{x}, \tilde{t}$ pair along its trajectory. Formally, the average of particle-labelled quantities is the ensemble average over all particles having the same labelling coordinates. In the statistically stationary case this is the time average over the temporal Lagrangian label and the result depends only on the difference between observation and labelling times. For example, $V(t - \tilde{t}|\tilde{x}) = \langle u(\tilde{t}|\tilde{x}, \tilde{t}) \rangle$ is the mean velocity at time t of all particles passing through $\tilde{x}, \tilde{t}$ and depends only on $t - \tilde{t}$. Note that $u'(\tilde{t}|\tilde{x}, \tilde{t})$ is the departure from $U(x)$, not V, along the $\tilde{x}, \tilde{t}$ trajectory so it is a mixed Eulerian-Lagrangian quantity.

a. The formal solution. Along particle paths the θ evolution equation (1.3) has the solution

$$\theta(\mathbf{x}, t) = \int_0^t q\{\mathbf{r}(\tilde{t}|\mathbf{x}, t), \tilde{t}\} d\tilde{t} + \theta\{\mathbf{r}(0|\mathbf{x}, t), 0\}$$

$$= \int_{-0}^t d\tilde{t} \int d\tilde{\mathbf{x}} \, \delta\{\tilde{\mathbf{x}} - \mathbf{r}(\tilde{t}|\mathbf{x}, t)\} \{q(\tilde{\mathbf{x}}, \tilde{t}) + \delta(\tilde{t})\theta(\tilde{\mathbf{x}}, 0)\}. \qquad (2.2)$$

The -0 lower limit denotes that the $\tilde{t}$ integration range includes the full width of $\delta(\tilde{t})$. For incompressible flow the Jacobian relating $\mathbf{x}$ and $\tilde{\mathbf{x}}$ is unity so that $\delta\{\tilde{\mathbf{x}} - \mathbf{r}(\tilde{t}|\mathbf{x}, t)\} = \delta\{\mathbf{x} - \mathbf{r}(\tilde{t}|\tilde{\mathbf{x}}, \tilde{t})\}$. Applying the filter $\langle \cdot \rangle$ to (2.2) gives

$$\Theta(\mathbf{x}, t) = \int_{-0}^t d\tilde{t} \int d\tilde{\mathbf{x}} \, C(\mathbf{x}, t - \tilde{t}, \tilde{\mathbf{x}}) \, \tilde{Q}(\tilde{\mathbf{x}}, \tilde{t}) \qquad (2.3a)$$

where

$$C(\mathbf{x}, t - \tilde{t}, \tilde{\mathbf{x}}) = \langle \delta\{\tilde{\mathbf{x}} - \mathbf{r}(\tilde{t}|\mathbf{x}, t)\} \rangle, \qquad (2.3b)$$

is the probability density of the position $\mathbf{x}$ at time t of those particles found at $\tilde{\mathbf{x}}, \tilde{t}$ and

$$\tilde{Q}(\mathbf{x}, t) = Q(\mathbf{x}, t) + \delta(t)\Theta(\mathbf{x}, 0)$$

combines the mean source Q and the initial Θ.

It must be noted that in applying the average $\langle \cdot \rangle$ to obtain (2.3) it was assumed that $q(\mathbf{x}, t)$ and $\theta(\mathbf{x}, 0)$ are independent of the fluctuations of fluid motion. Thus $t = 0$ is a special time and θ must be a strictly passive tracer. Vorticity and potential vorticity are dynamically related to velocity, so these quantities cannot be expected to evolve according to (2.3); Holloway and Kristmannsson (1984) presented a graphic example of the differing initial evolution of vorticity and passive tracers in geostrophic turbulence. In the same way, vertical transport of constituents such as temperature or salinity which affect density will not be well described by (2.3). Consideration of active tracers is beyond the scope of this paper.

Interpretation of (2.3) is straightforward. $C(\mathbf{x}, t - \tilde{t}, \tilde{\mathbf{x}})d\tilde{\mathbf{x}}$ is the transition probability that the particle at $\mathbf{x}, t$ came from the region $d\tilde{\mathbf{x}}$ surrounding $\tilde{\mathbf{x}}$ at time $\tilde{t}$; in incompressible flow this is equal to the probability that the particle from $\tilde{\mathbf{x}}, \tilde{t}$ went to $d\tilde{\mathbf{x}}$ around $\mathbf{x}$ at t. As a function of $\mathbf{x}$, $C(\mathbf{x}, t - \tilde{t}, \tilde{\mathbf{x}})$ is the concentration at time t of those particles which pass through $\tilde{\mathbf{x}}, \tilde{t}$. For $t > \tilde{t}$ this could be determined from the average density at time t of particles released at $\tilde{\mathbf{x}}, \tilde{t}$. For $t > \tilde{t}$ there is no simple experiment to find $C(\mathbf{x}, t - \tilde{t}, \tilde{\mathbf{x}})$ as a function of $\tilde{\mathbf{x}}$.

Formally, (2.3) specifies the mean field Θ in terms of the mean initial and source fields and the complete statistical description of single Lagrangian particles. This "solution" is conceptually opaque, not even providing a framework for separating advection from eddy transport, and has no predictive ability until C is known. Its major utility is in casting the mean property transport problem into the language of

observable particle motion where physically motivated approximations are more easily introduced.

Although the transition probability density $C(\mathbf{x}, t, \tilde{\mathbf{x}})$ could, in principle, be observed it would require an unreasonable number of observations to do so. Direct observation of $C(\mathbf{x}, t \, \tilde{\mathbf{x}})$ would involve dividing the region of interest in M spatial resolution cells of, say equal, areas $a(\mathbf{x})$. Then for every time lag t the fraction of particles arriving in any $a(\mathbf{x})$ from each $a(\tilde{\mathbf{x}})$ would be $C(\mathbf{x}, t, \tilde{\mathbf{x}})a(\tilde{\mathbf{x}})$. From a sample of N particles in $a(\mathbf{x})$ the sampling error for C would be (*cf.* Bendat and Piersol, 1971, §6.3.1)

$$\delta C = \frac{C}{\{NCa\}^{1/2}}$$

where NCa will be recognized as the expected number of particles to have come from $a(\tilde{\mathbf{x}})$.

For C to be useful the error δC should be much smaller than the larger of C itself or $1/Ma$, the density corresponding to a uniform source distribution over the M areas. Meeting $\delta C < \epsilon C$ or $\delta C < \epsilon/Ma$ for all C values requires $N > M/\epsilon^2$ samples in each of the M destination regions. If the particle velocity decorrelation time is τ, and the time ranges t of interest are larger than τ, then the decorrelation time for the displacements of interest is $O(t)$ and a total data set of tM^2/ϵ^2 particle time units would be required. This is larger by a factor of Mt/τ than the data set required to observe a diffusivity in each of M regions with fractional error ϵ. This extra factor even makes observing C in a numerical model an impractically large problem.

The purpose of a Θ evolution equation, such as the advection plus eddy diffusion model, is to replace the spatially and temporally global specification (2.3) with something which is accurate enough to be predictive, is conceptually useful, and involves only observable transport parameters. Since it is not practical to observe the transition probability and (2.3) is not conceptually useful in describing transport, the remainder of this section concerns conversion of the spatially and temporally global integral of (2.3) into a useful transport model.

Time differentiation of (2.3a) followed by use of (2.1) and (2.3b) gives

$$\partial_t \Theta(\mathbf{x}, t) + \mathbf{U}(\mathbf{x}) \cdot \nabla \Theta(\mathbf{x}, t) = Q(\mathbf{x}, t) - \nabla \cdot \mathbf{E}(\mathbf{x}, t) \tag{2.4a}$$

where

$$\mathbf{E}(\mathbf{x}, t) = \int_{-0}^{t} d\tilde{t} \int d\tilde{\mathbf{x}} \, \mathbf{e}(\mathbf{x}, t - \tilde{t}, \tilde{\mathbf{x}}) \, \tilde{Q}(\tilde{\mathbf{x}}, \tilde{t}) \tag{2.4b}$$

$$\mathbf{e}(\mathbf{x}, t - \tilde{t}, \tilde{\mathbf{x}}) = \langle \mathbf{u}'(\mathbf{x}, t)\delta\{\tilde{\mathbf{x}} - \mathbf{r}(\tilde{t}|\mathbf{x}, t)\}\rangle. \tag{2.4c}$$

$\mathbf{E}$ is the eddy flux of θ-stuff while $\mathbf{e}(\mathbf{x}, t - \tilde{t}, \tilde{\mathbf{x}})$ is the eddy flux through $\mathbf{x}, t$ of particles from $\tilde{\mathbf{x}}, \tilde{t}$.

In order to use (2.4) it is necessary to relate the eddy fluxes $\mathbf{E}$ and $\mathbf{e}$ to mean field

quantities Θ and C, respectively. The approach here is to use a simple, if unusual, model of particle motion to do this.

b. Particle motion model. The central element of this development is a statistically optimized model for predicting a particle's trajectory from knowledge of its position $\mathbf{x}$ at time t and of its velocity at that time. Define

$$\mathbf{s}(\tilde{t}|\mathbf{x}, t) = \mathbf{r}(\mathbf{t}|\mathbf{x}, t) - \mathbf{r}(\tilde{t}|\mathbf{x}, t) = \mathbf{x} - \mathbf{r}(\tilde{t}|\mathbf{x}, t)$$

to be the displacement from time $\tilde{t}$ to t of the particle found at $\mathbf{x}, t$. The most general linear model for $\mathbf{s}$ is

$$s_m(\tilde{t}|\mathbf{x}, t) = \alpha_{mk}(\mathbf{x}, t - \tilde{t})u'_k(\mathbf{x}, t) + \chi_m(\tilde{t}|\mathbf{x}, t) \qquad (2.5a)$$

where here and below the repeated index sum convention is implied. The remainder χ has a mean part and a fluctuation which is taken to be unpredictable. We seek the model which minimizes the unpredictable part of χ in the least mean square sense, that is the α *vs.* t which minimizes

$$\langle |\chi - \langle \chi \rangle|^2 \rangle = \langle |\mathbf{s}' - \alpha \cdot \mathbf{u}'|^2 \rangle = \langle s'_n s'_n \rangle - 2\alpha_{nk}\langle s'_n u'_k \rangle + \alpha_{nk}\alpha_{nl}\langle u'_k u'_l \rangle.$$

This quadratic form for α is minimized by the α which extremizes it, that is

$$\alpha_{mk}(\mathbf{x}, t - \tilde{t}) = D_{kn}^{-1}(\mathbf{x})\kappa_{nm}(\mathbf{x}, t - \tilde{t}) \qquad (2.5b)$$

where

$$D_{kn}(\mathbf{x}) = \langle u'_k(\mathbf{x}, t)u'_n(\mathbf{x}, t) \rangle \qquad (2.5c)$$

is the Eulerian covariance of $\mathbf{u}'$ and

$$\kappa_{nm}(\mathbf{x}, t) = \langle u'_n(\mathbf{x}, t)s_m(0|\mathbf{x}, t) \rangle = \int_0^t dt_1 \langle u'_n(\mathbf{x}, t)u_m(t_1|\mathbf{x}, t) \rangle. \qquad (2.5d)$$

If there is some time lag τ beyond which the velocity mean product in (2.5d) vanishes then

$$\kappa(\mathbf{x}, t) = \kappa^\infty(\mathbf{x}) \qquad \text{for } t > \tau. \qquad (2.5e)$$

The component of the total displacement $\mathbf{s}$ which is predictable from a single velocity plays a central role in what follows. It is specially denoted

$$\tilde{\mathbf{s}}(\tilde{t}|\mathbf{x}, t) = \alpha(\mathbf{x}, t - \tilde{t}) \cdot \mathbf{u}'(\mathbf{x}, t). \qquad (2.5f)$$

Since

$$\langle \tilde{s}_n \tilde{s}_m \rangle = \alpha_{nk}\alpha_{mj}D_{kj} = \alpha_{nk}\kappa_{km}, \qquad (2.5g)$$

the typical size of $\tilde{\mathbf{s}}$ ceases to grow for time lags beyond τ.

The model (2.5) is the kind of so-called optimal estimator frequently used in data

analysis (e.g. in objective mapping). It may be regarded as a statistically corrected form of the approximation $s(0|\mathbf{x}, t) = \int_0^t dp\, \mathbf{u}(\mathbf{x}, p)$ used in predicting Stokes drift in wave fields. Here it is recognized that no exact linear relation exists between s and u and the statistically best approximation is employed. In philosophy at least, this approach is related to quasi-normal Markovian models where a nonlinear evolution equation is modeled by a linear one driven by normally distributed random forcing. Here the linear model is not explicitly stated but rather is implied by its transfer function $\alpha(\mathbf{x}, t)$. The assumption below that χ' is strictly unpredictable takes the place of the normally distributed forcing proviso, although it is not equivalent in detail.

Within the context of the model (2.5), the single-particle diffusivity κ relates a particle's displacement to its instantaneous velocity. The diffusivity predicts both where a particle will go and where it came from. So long as $\kappa(\mathbf{x}, t)$ does not vanish, a particle's velocity provides some predictability of its displacement over time range t. It is this predictability at large time ranges which leads to diffusive transport. The diffusivity definition in (2.5d) differs from the more common diffusivity defined by Taylor (1921); the Taylor diffusivity is a pure Lagrangian statistic while κ is a mixed Eulerian-Lagrangian statistic involving $\mathbf{u}'$, the departure from the Eulerian mean velocity. Taylor's diffusivity was intended to apply to statistically homogeneous situations and in that case the two definitions coincide. This is most easily seen in the one-dimensional case with no mean flow when (2.5d) is

$$\kappa(x, t) = \langle u(x, t_0)\{r(t_0|x, t_0) - r(t_0 - t|x, t_0)\}\rangle$$

and the Taylor diffusivity is

$$K(\tilde{x}, t) = \langle u(t + \tilde{t}|\tilde{x}, \tilde{t})\{r(t + \tilde{t}|\tilde{x}, \tilde{t}) - r(\tilde{t}|\tilde{x}, \tilde{t})\}\rangle.$$

For statistically homogeneous cases averaging can be extended over x since κ is independent of x. Thus particles in the Taylor definition can be relabelled according to $\hat{x} = r(t + \tilde{t}|\tilde{x}, \tilde{t})$, $t_0 = t + \tilde{t}$ to convert the definition of $K(t)$ to the one for $\kappa(t)$. Thus (2.5d) may be regarded as a generalization of the Taylor diffusivity to statistically inhomogenous flows.

Using the particle motion model (2.5), a simple relation between $\mathbf{E}$ and Θ is obtained under two different sets of restrictions. In one, conditions are placed on the spatial of $\tilde{Q}$ and the spatial variations of particle displacement statistics. In the other, the turbulent velocity $\mathbf{u}'$ is taken to have an approximately Gaussian probability density and restrictions are placed on the spatial variation of particle displacement statistics. In both developments the lack of correlation between $\mathbf{u}'(\mathbf{x}, t)$ and $\chi(\tilde{t}|\mathbf{x}, t)$ in the model (2.5) is taken to imply that they may be treated as statistically independent. Notation is simplified by suppressing the arguments of $\mathbf{u}'(\mathbf{x}, t)$, $\alpha(\mathbf{x}, t - \tilde{t})$, $\chi(\tilde{t}|\mathbf{x}, t)$, and $\tilde{s}(\tilde{t}|\mathbf{x}, t)$. L^Q is taken to be the spatial scale over which $\tilde{Q}$ varies and L^x is the scale over which the particle statistics $\langle \chi^2 \rangle$ and $\langle \tilde{s}^2 \rangle$ vary.

c. Scale separation. The trajectory prediction model (2.5) can be used to write (2.3) and (2.4) as

$$\begin{bmatrix} \Theta(\mathbf{x}, t) \\ E(\mathbf{x}, t) \end{bmatrix} = \int_{-0}^{t} d\tilde{t} \left\langle \begin{bmatrix} 1 \\ \mathbf{u}' \end{bmatrix} \tilde{Q}(\mathbf{x} - \alpha \cdot \mathbf{u}' - \chi, \tilde{t}) \right\rangle, \qquad (2.6a)$$

where the average is over all values of $\mathbf{u}'$ and χ, which are assumed statistically independent. If $\tilde{s} = \alpha \cdot \mathbf{u}'$ is much smaller than $L^{Q} + \langle \chi^2 \rangle^{1/2}$ then $\tilde{Q}$ can be expanded around $\mathbf{x} - \chi$ to give

$$E_n(\mathbf{x}, t) = - \int_{-0}^{t} d\tilde{t} \, \kappa_{nm}(\mathbf{x}, t - \tilde{t}) \left\langle \left[\frac{\partial \tilde{Q}(\mathbf{p} - \chi, \tilde{t})}{\partial p_m} \right]_{\mathbf{p} - \mathbf{x}} \right\rangle. \qquad (2.6b)$$

The derivative in (2.6b) is not simply ∂_x because the statistics of χ may depend on x. If the statistics are homogeneous then the average of $\tilde{Q}(\mathbf{p} - \chi)$ will not depend on x and the derivative becomes a simple x-derivative. In general

$$\left\langle \frac{\partial \tilde{Q}(x - \chi)}{\partial x_m} \right\rangle = \left\langle \left[\frac{\partial \tilde{Q}(\mathbf{p} - \chi)}{\partial p_n} \right]_{\mathbf{p} - \mathbf{x}} \left[\delta_{nm} - \frac{\partial \chi_n}{\partial x_m} \right] \right\rangle.$$

The typical size of $\partial_x \chi$ is $\langle \chi^2 \rangle^{1/2} / L^x$ so that if $L^x \gg \langle \chi^2 \rangle^{1/2}$ then

$$E_n(\mathbf{x}, t) = - \int_{-0}^{t} d\tilde{t} \, \kappa_{nm}(\mathbf{x}, t - \tilde{t}) \frac{\partial}{\partial x_m} \langle \tilde{Q}(\mathbf{x} - \chi, \tilde{t}) \rangle. \qquad (2.6c)$$

Integrating this by parts and noting the definition of Θ in (2.6a) leads to the elaborated flux *vs.* gradient law

$$E_n(\mathbf{x}, t) = - \kappa_{nm}(\mathbf{x}, t) \frac{\partial}{\partial x_m} \Theta(\mathbf{x}, t)$$

$$\qquad\qquad - \int_{-0}^{t} d\tilde{t} \frac{\partial \kappa_{nm}(\mathbf{x}, t - \tilde{t})}{\partial \tilde{t}} \frac{\partial}{\partial x_m} [\Theta(\mathbf{x}, t) - \Theta(\mathbf{x}, \tilde{t})] \qquad (2.7a)$$

$$\qquad\qquad = - \int_{-0}^{t} d\tilde{t} \frac{\partial \kappa_{nm}(\mathbf{x}, t - \tilde{t})}{\partial t} \frac{\partial \Theta(\mathbf{x}, \tilde{t})}{\partial x_m}$$

$$\qquad\qquad = - \int_{-0}^{t} d\tilde{t} \frac{\partial \kappa_{nm}(\mathbf{x}, \tilde{t})}{\partial \tilde{t}} \frac{\partial \Theta(\mathbf{x}, t - \tilde{t})}{x_m}. \qquad (2.7b)$$

The flux law (2.7) is the major theoretical result of this paper. It specifies the flux of a passive scalar from the recent history of its mean concentration. The driving force for the eddy flux at time t is the sum of previous Θ gradients at times $t - \tilde{t}$ weighted by the time derivative of κ at time range $\tilde{t}$. This is an elaboration of the familiar eddy diffusion model, the elaboration reflecting the finite scales of the dispersing eddies. For $t > \tau$ the diffusivity in the flux *vs.* gradient part of (2.7a) becomes constant and the second term depends only on the recent history of Θ for times between $t - \tau$ and t. If Θ does not vary

over that time range, this extra "history" term vanishes, the eddy flux is simply proportional to the mean gradient, and Θ evolves according to a pure advection-diffusion equation with the constant eddy diffusivity $\kappa^\infty(\mathbf{x})$.

The development above is similar to the conventional justification of a diffusive flux law (*cf.* the Appendix). It is based on the particle displacement being small, specifically

$$\langle \tilde{\jmath}^2 \rangle^{1/2} \ll L^\varrho + \langle \chi^2 \rangle^{1/2} \qquad \text{and} \qquad \langle \chi^2 \rangle^{1/2} \ll L^\chi. \tag{2.8}$$

The first of these is straightforward because $\langle \tilde{\jmath}^2 \rangle^{1/2}$ reaches an asymptotic value which L^ϱ must exceed. The second is more difficult to assess because both the mean square and inhomogeneity scale of $\chi(\tilde{t}|\mathbf{x}, t)$ depend on $t - \tilde{t}$. We note that the flux law (2.7) depends on the history of Θ, but only over $t > \tilde{t} > t - \tau$. Thus if the restrictions (2.8) apply for $t - \tilde{t} \le O(\tau)$ then the flux law (2.7) must apply for all t because the equation itself contains no reference to the initial time $t = 0$ once κ has reached its asymptotic value. In essence the solution for large time t can be obtained by reinitializing (2.7) at any time previous to $t - \tau$.

d. Gaussian $\mathbf{u}'$. Because $\mathbf{u}'$ and χ are treated as statistically independent, (2.3) and (2.4) can be written as

$$\begin{bmatrix} \Theta(\mathbf{x}, t) \\ E(\mathbf{x}, t) \end{bmatrix} = \int_{-0}^{t} d\tilde{t} \int d\hat{\mathbf{x}} \left\langle \begin{bmatrix} 1 \\ \mathbf{u}' \end{bmatrix} \delta(\hat{\mathbf{x}} - \mathbf{x} + \alpha \cdot \mathbf{u}') \right\rangle \langle \tilde{Q}(\hat{\mathbf{x}} - \chi) \rangle; \tag{2.9a}$$

the first average is over values of $\mathbf{u}'$ and the second is over χ. The average over $\mathbf{u}'$ can be evaluated from the probability density of $\mathbf{u}'$. Suppose this probability density $G(\mathbf{u}'; \mathbf{x})$ has an approximately Gaussian form so that

$$u'_n G(\mathbf{u}') \approx D_{nm} \frac{\partial G(\mathbf{u}')}{\partial u_m}$$

where D is the velocity covariance of (2.5c). Then

$$\langle u'_n \delta(\hat{\mathbf{x}} - \mathbf{x} + \alpha \cdot \mathbf{u}') \rangle = -D_{nm} \int d\mathbf{u} \frac{\partial G}{\partial u_m} \langle \delta(\hat{\mathbf{x}} - \mathbf{x} + \alpha \cdot \mathbf{u}') \rangle$$

$$= \kappa_{nm}(\mathbf{x}, t - \tilde{t}) \frac{\partial}{\partial \hat{x}_m} \langle \delta(\hat{\mathbf{x}} - \mathbf{x} + \alpha \cdot \mathbf{u}') \rangle. \tag{2.9b}$$

This is a valid approximation so long as the higher cumulants of $\mathbf{u}'$ are small compared with the appropriate powers of the covariance D.

If the statistics of the predictable displacement $\tilde{\mathbf{s}} = \alpha \cdot \mathbf{u}'$ vary on the scale L^χ and if $\langle \tilde{\jmath}^2 \rangle^{1/2} \ll L^\chi$ then

$$\frac{\partial}{\partial \hat{x}_m} \langle \delta(\hat{\mathbf{x}} - \mathbf{x} + \alpha \cdot \mathbf{u}') \rangle \approx -\frac{\partial}{\partial x_m} \langle \delta(\hat{\mathbf{x}} - \mathbf{x} + \alpha \cdot \mathbf{u}') \rangle.$$

In a statistically homogeneous situation this relation is exact because neither α nor the statistics of $\mathbf{u}'$ depend on $\mathbf{x}$. Similarly, in a statistically homogeneous situation $\langle \tilde{Q}(\hat{\mathbf{x}} - \chi) \rangle$ does not depend on $\mathbf{x}$; even though χ is a function of $\mathbf{x}$, its statistics are not. In general

$$\frac{\partial}{\partial x_n} \langle \tilde{Q}(\hat{\mathbf{x}} - \chi) \rangle = \left\langle \frac{\partial \tilde{Q}(\hat{\mathbf{x}} - \chi)}{\partial \hat{x}_m} \frac{\partial \chi_m}{\partial x_n} \right\rangle = O\left[\frac{\tilde{Q}}{L_m^Q + \langle \chi_m^2 \rangle^{1/2}} \frac{\langle \chi_m^2 \rangle^{1/2}}{L_n^x} \right].$$

Note that the scale of $\langle \tilde{Q}(\mathbf{x} - \chi) \rangle$ exceeds L^Q by the typical size of χ.

The scale of $\langle \delta(\hat{\mathbf{x}} - \mathbf{x} + \alpha \cdot \mathbf{u}') \rangle$ is $\langle \mathfrak{s}^2 \rangle^{1/2}$ so that we may write, from (2.9a) and (2.9b),

$$\langle u_n' \delta(\hat{\mathbf{x}} - \mathbf{x} + \alpha \cdot \mathbf{u}') \rangle \langle \tilde{Q}(\hat{\mathbf{x}} - \chi) \rangle$$

$$\approx - \kappa_{nm}(\mathbf{x}, t - \tilde{t}) \frac{\partial}{\partial x_m} [\langle \delta(\hat{\mathbf{x}} - \mathbf{x} + \alpha \cdot \mathbf{u}') \rangle \langle \tilde{Q}(\hat{\mathbf{x}} - \chi) \rangle] \quad (2.9c)$$

so long as

$$\langle \mathfrak{s}^2 \rangle^{1/2} \ll L^x \qquad \text{and} \qquad \langle \mathfrak{s}_n^2 \rangle^{1/2} \langle \chi_m^2 \rangle^{1/2} \ll L_n^x (L_m^Q + \langle \chi_m^2 \rangle^{1/2}). \quad (2.9d)$$

The second of these compares with the restriction on L^Q in (2.8). In this case, however, if the first restriction is met then the second follows automatically.

Substitution of (2.9c) into (2.9a) followed by parts integration over $\tilde{t}$ again yields the elaborated flux *vs.* gradient relation (2.7).

e. Transport of Θ. Both the above developments lead to the eddy flux law (2.7) and, consequently, the Θ-stuff transport equation

$$\partial_t \Theta(\mathbf{x}, t) + \mathbf{U}(\mathbf{x}) \cdot \nabla\Theta(\mathbf{x}, t) - Q(\mathbf{x}, t)$$

$$= \nabla \cdot \kappa(\mathbf{x}, t) \cdot \nabla\Theta(\mathbf{x}, t) + \nabla \cdot \int_{-0}^{t} d\tilde{t} \frac{\partial \kappa(\mathbf{x}, t - \tilde{t})}{\partial \tilde{t}} \cdot \nabla[\Theta(\mathbf{x}, t) - \Theta(\mathbf{x}, \tilde{t})]$$

$$= \nabla \cdot \int_{-0}^{t} d\tilde{t} \frac{\partial \kappa(\mathbf{x}, \tilde{t})}{\partial \tilde{t}} \cdot \nabla\Theta(\mathbf{x}, t - \tilde{t}). \quad (2.10)$$

Because the diffusivity κ depends on time, the eddy flux of Θ depends on the history of $\nabla\Theta$, not just its present value. If κ were independent of time, then the right hand side of (2.10) would reduce to $\nabla \cdot \kappa \cdot \nabla\Theta$ and Θ would evolve by advection plus diffusion. If κ reaches its asymptotic value quickly, as it does in the molecular diffusion case, the extra "history" term is negligible.

The transport model (2.10) is valid under two sets of restrictions:

$$\langle \mathfrak{s}^2 \rangle^{1/2} \ll L^Q + \langle \chi_r^2 \rangle^{1/2} \qquad \text{and} \qquad \langle \chi_r^2 \rangle^{1/2} \ll L^x, \quad (2.11a,b)$$

or

$$\mathbf{u}' \text{ is Gaussian} \qquad \text{and} \qquad \langle \mathfrak{s}^2 \rangle^{1/2} \ll \langle L^x \rangle. \quad (2.12a,b)$$

In scale-separation restriction (2.11) $\chi_\tau = \chi(t - \tau|\mathbf{x}, t)$, the unpredictable displacement over time lag τ. The scale restrictions (2.11) can be much more stringent than (2.12). First, (2.12) places no restrictions on the scale of Q; evidently the Gaussian-$\mathbf{u}'$ condition avoids the requirement invoked in heuristic developments of the eddy diffusion flux law that the scale of Θ be large. Second, the displacement $\chi\tau$, includes the mean particle displacement and may, therefore, be much larger than $\tilde{\mathfrak{s}}$, making (2.11b) much more stringent than (2.12b). The stringency of the conditions (2.11) and (2.12) is addressed further in the following section.

It may appear surprising that the normally distributed $\mathbf{u}$ assumption is important in determining the form of the Θ evolution equation. Recall, however, that normally distributed displacements are an integral part of the random walk processes producing diffusion. Here displacements over short times are normally distributed only if $\mathbf{u}$ is normally distributed. Evidently, normally distributed displacements lead to much less strigent scale separation restrictions on diffusive eddy transport laws and their elaborations.

Suppose that for some $t > \tau$ the time scale, T_Θ, of Θ becomes great enough that a two term Taylor series expansion about t is adequate to describe $\Theta(\mathbf{x}, \tilde{t})$ over $t - \tau < \tilde{t} < t$. Then

$$E_n = -\kappa_{nm}^\infty \frac{\partial\Theta}{\partial x_m} + \mu_{nm} \frac{\partial^2\Theta}{\partial x_m \partial t}, \qquad \mu_{nm}(\mathbf{x}, t) = \int_0^t \frac{\partial\kappa_{nm}(\mathbf{x}, \tilde{t})}{\partial \tilde{t}} \cdot \tilde{t} \cdot d\tilde{t}, \qquad (2.13a)$$

and the history term contributes an $O(\tau|T_\Theta)$ fraction to the eddy flux. In an initial value problem, the history contribution will presumably become negligible after some time. This does not, however, imply that Θ predicted by an advection-diffusion model will be accurate at this time; the effect on Θ of earlier history correction to $\mathbf{E}$ will persist beyond the time a simple flux *vs.* gradient law pertains.

The structure of the history correction to $\mathbf{E}$ can be seen by writing (2.13a) as

$$E_n(\mathbf{x}, t) = -\sum_m \kappa_{nm}^\infty(\mathbf{x}) \frac{\partial}{\partial x_m} \Theta(\mathbf{x}, t - \tau_{nm}) \qquad \text{where} \qquad \tau_{nm}(\mathbf{x}) = \frac{\mu_{nm}(\mathbf{x})}{\kappa_{nm}^\infty(\mathbf{x})}; \quad (2.13b)$$

there are no implied sums in (2.13b). If κ approaches κ^∞ without overshooting, then μ_{nm} will be of the same sign as κ_{nm}^∞, the τ_{nm}'s will be positive, and the flux $\mathbf{E}$ at time t will be proportional to the gradient of Θ at earlier times. It is possible, if pathological, for the times τ_{nm} to be negative.

We close this section with a review of the structure and implicit restrictions of the development leading to the elaborated advection-diffusion model (2.10). The development is based on rational approximation of the particle statistics determining $C(\mathbf{x}, t - \tilde{t}, \tilde{\mathbf{x}})$ which describes the probability that a particle found at $\mathbf{x}$, t was near $\tilde{\mathbf{x}}$ at $\tilde{t}$. Evolution of C is described by (2.4), which involves the advective flux $\mathbf{U}C$ and an eddy flux.

The approach here is based on a statistically optimized linear estimator to predict

particle's displacement from its velocity at one time. The linear estimator naturally introduces the single-particle diffusivity $\kappa(\mathbf{x}, t)$ of (2.5). This mixed Eulerian-Langrangian statistic is the mean product of a particle's displacement and the velocity perturbation from the Eulerian mean at one end of the trajectory. This differs from the more usual definition of the diffusivity which does not involve the perturbation from the Eulerian mean. Interest here is in the "backward looking" diffusivity relating a particles previous displacement to its present velocity perturbation.

Two sets of restrictions lead to an elaborated eddy diffusion law for the eddy flux of Θ. One places fairly stringent limits on the size of particle displacements over the Lagrangian velocity decorrelation time scale τ as compared with both the spatial scales over which Θ and particle motion statistics vary. The other leads to less restrictive conditions on the particle displacement as compared with particle statistics inhomogeneity scales, but requires the turbulent velocity to have an approximately normal probability distribution. We turn now to examining how stringent these requirements are.

3. Numerical experiments

The development in the previous section led to the elaborated eddy diffusion model (2.10) for the evolution of Θ. In this model the eddy flux $\mathbf{E}$ is determined by the recent history of the gradient of Θ and the time-dependent single-particle diffusivity

$$\kappa_{nm}(\mathbf{x}, t - \tilde{t}) = \langle u'_n(\mathbf{x}, t) s_m(\tilde{t} | \mathbf{x}, t) \rangle \tag{3.1}$$

where

$$\mathbf{s}(\tilde{t} | \mathbf{x}, t) = \mathbf{x} - \mathbf{r}(\tilde{t} | \mathbf{x}, t)$$

is the displacement the particle found at $\mathbf{x}, t$ undergoes from time $\tilde{t}$ to time t. Transport is determined by $\kappa(\mathbf{x}, t)$ which approaches the asymptotic value $\kappa^{\infty}(\mathbf{x})$ for $t > \tau$.

The theoretical development is based on the restrictions (2.11) or (2.12) being met. These concern the typical size of the displacement $\tilde{s}$ which is predictable from $\mathbf{u}'(\mathbf{x}, t)$, the size of the unpredictable part of displacement, $\chi(\tilde{t} | \mathbf{x}, t)$, and the probability density of $\mathbf{u}'(\mathbf{x}, t)$. The purpose of this section is to see how stringent these restrictions are in fields of simulated geophysical turbulence. Additionally, the effect of variation of Coriolis' parameter, mean velocity shear and confining boundaries on property transport will be seen; the intent is not to parameterize κ but simply to explore qualitatively the effect of these physical quantities.

a. Description of the experiments. Realizations of idealized one-layer quasi-geostrophic turbulence were constructed from a conventional 64×64 pseudo-spectral model of

$$\partial_t \zeta + \mathbf{u} \cdot \nabla(\zeta + \beta y) = -\nu \nabla^4 \zeta - \gamma \zeta + \epsilon F, \qquad \zeta = \nabla \times \mathbf{u} = -\nabla^2 \psi \tag{3.2}$$

where F is a random torque used to maintain turbulence and ψ is the streamfunction of the velocity **u**. Vorticity was advanced numerically using an explicit centered time difference (leap-frog) scheme with smoothing every 2000 steps. Particle trajectories were computed using a second order interpolation of velocity from the computational grid; this interpolation fits the velocity at the grid point nearest the particle and the four nearest neighbors of that point. Particle positions were advanced using a second order Runge-Kutta scheme. Various experiments were carried out, each over a statistically steady time range of 32 during which 64 widely spaced particles were tracked. Eulerian and Lagrangian statistics were computed from these data.

Results are reported in terms of variables made dimensionless using the width of the computational domain L_c, the characteristic velocity U_c, and the time $T_c = L_c/U_c$. The forcing F had unit variance, a wavenumber spectrum which is white over the wavenumber range $6 \times 2\pi \leq k_x$, $k_y \leq 8 \times 2\pi$, a temporal correlation which decayed exponentially (F is a first order Markov process) with a scale of one time unit, and a Gaussian distribution. Lateral damping was minimized subject to the requirement that enstrophy not accumulate at high k. The forcing amplitude ϵ and the drag γ were adjusted to set the total kinetic energy near unity and shape the energy spectrum.

Four experiments are reported: fP is the basic f-plane experiment with $\beta = 0$, no mean flow, and periodic boundary conditions at $x = 0, 1$ and $y = 0, 1$; βP is the same situation with $\beta = 820$ corresponding to a small β-Rossby number; SHR is like fP except that the mean shear $U = \sin(2\pi y)$ is imposed; WALL is like fP except that no-normal-flow no-shear boundary conditions ($\psi = \partial_{yy}^2\psi = \partial_{yyyy}^4\psi = 0$) are imposed at $y = 0$ and $y = 0.5$; the higher order boundary condition is a consequence of the

Table 1. Parameters for experiments reported here and VO2 from Haidvogel and Keffer (1984). Runs reported here used a biharmonic viscosity $\nu = 7.6 \times 10^{-8}$ while VO2 used harmonic lateral damping. β is the dimensionless gradient of the Coriolis parameter (inverse β-Rossby number) in (3.2). $\langle u'^2 \rangle$ is the eddy kinetic energy (excluding the mean flow in SHR). $T_{\zeta} = \langle \zeta'^2 \rangle^{-1/2}$ is the eddy turnover time. $T_\gamma = 1/\gamma$ is the "bottom friction" damping time. $T_\nu = (\nu k_{\zeta}^4)^{-1}$ is the lateral friction damping time at the characteristic energy wavenumber $k_{\zeta} = (\langle \zeta'^2 \rangle/\langle u'^2 \rangle)^{1/2}$; for VO2 $T_\nu = (\nu k_{\zeta}^2)^{-1}$. $T_{MAX} = (\nu k_{MAX}^4)^{-1}$ is the lateral damping time at the highest resolved wavenumber k_{MAX}; for VO2 $T_{MAX} = (\nu k_{MAX}^2)^{-1}$. ϵ is the strength of the random torque used to excite turbulence. Eddy statistics are reasonably homogeneous across the SHR domain. For WALL statistics are reasonably homogeneous over the 85% of the domain away from the walls; quoted values are for this region.

	fP	βP	SHR	WALL	VO2
$\langle u'^2 \rangle$	0.97	0.97	0.46	1.10	1.3
β	0	820	0	0	395
T_{ζ}	0.026	0.027	0.035	0.025	0.019
T_γ	1.6	1.6	0.8	1.6	1.6
T_ν	6.3	6.3	4.2	5.7	2.9
T_{MAX}	0.008	0.008	0.008	0.008	0.24
ϵ	0.18	0.18	0.16	0.18	—

Journal of Marine Research

psuedo-spectral representation used. The parameters for these experiments are given in Table 1 along with some derived measures which can be used to compare with models using different parameterizations; included in the table are values from Haidvogel and Keffer's (1984) experiment VO2 in which particle motion was simulated.

Figure 1 presents the scalar wavenumber spectra $S_u(k)$, $S_v(k)$ and $S_\zeta(k)$ of velocities u', v' and vorticity ζ', respectively. These have similar structure for all experiments, all being dominated by low-k velocity, all exhibiting an enstrophy peak at k's slightly above those excited by random forcing, and all having a featureless cascade beyond this enstrophy peak with a spectral slope near k^{-5} or k^{-6}. Differences between the experiments are observed primarily at low-k where βP shows a relative deficit of energy and both βP and SHR are anisotropic with βP dominated by u' and SHR showing a slight excess of v' energy.
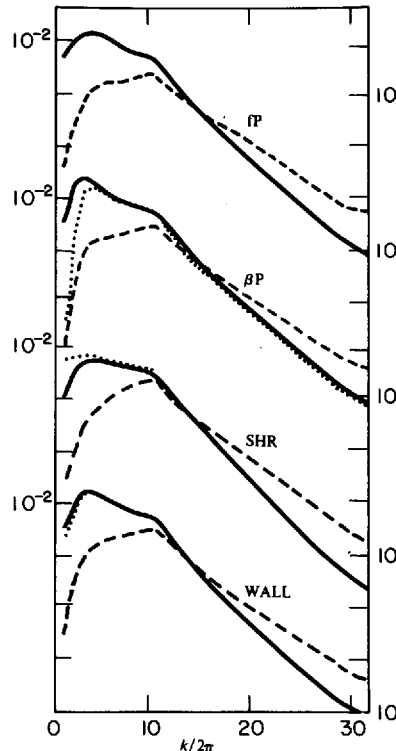

Figure 1. Scalar wavenumber spectra of u' (solid), v' (dotted), and ζ' (dashed) determined from the variance of Fourier coefficients of streamfunction. For example the spatial and temporal average variance of u' is the integral of the u' spectrum from $k = 0$ to $k - 64\pi$ where $k = |\mathbf{k}|$. The logarithmic scales for each experiment listed in Table 1 are offset by three decades. The u' and v' scales are on the left and the ζ' scale is on the right. The energy of the mean flow is excluded from the SHR spectra.
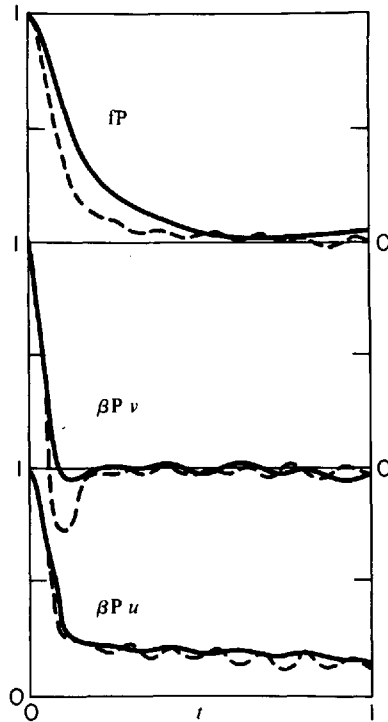
Figure 2. Eulerian average (solid) and Lagrangian average (dashed) time-lagged velocity correlations for fP and βP. The Eulerian correlation is $\langle u'(\mathbf{x}, t_0)u'(\mathbf{x}, t + t_0)\rangle \mid \langle u'^2\rangle$ where the average is over $\mathbf{x}$ and t_0. The Lagrangian correlation is $\langle u'(\mathbf{x}, t_0)\{u(t + t_0|\mathbf{x}, t_0) - V_x(t)\}\rangle$ normalized by the appropriate standard deviations. While $\mathbf{V}(0) = \mathbf{U} = 0$, over longer displacement times there is apparently a small Stokes Drift in βP leading to $V_x \approx -0.06$ but determination of $\mathbf{V}$ is uncertain because of the long time scale of u'.

Figure 2 presents the Eulerian and Lagrangian averaged time-lagged correlations of velocity for the homogeneous runs fP and βP. In fP the Eulerian time scale is substantially longer than the Lagrangian time scale; this has been observed in other simulations (Davis, 1982 and 1983) and in drifter observations of coastal currents (Davis, 1985) but contrasts with the finding of Freeland *et al.* (1975) that the Eulerian and Lagrangian time scales were nearly equal for mid-depth velocities in a field dominated by mesoscale eddies. In βP the Eulerian and Lagrangian time scales are comparable and are significantly shorter than those in fP. There is substantial anisotropy in βP and much of the u' energy is in very low frequency motion. Apparently low β-Rossby number turbulence is dominated at low frequency by zonal variability. From the practical vantage of measuring flow statistics, these low frequency motions substantially increase the length of observation required to achieve an accurate estimate.

It is hypothesized that the Lagrangian time scale in fP is shorter than the Eulerian

time scale because particles are swept through the relatively stationary f-plane turbulence faster than the eddies evolve at one point. The large β in βP leads to a substantially more rapid decorrelation of velocity than in fP, presumably because the turbulence takes on Rossby wave characteristics and propagates. In fact the spectrum of v' has a clear peak at $\omega \approx 30$ which corresponds in the Rossby wave dispersion curve to wavenumbers near the peak of the $S_u(k)$ and $S_v(k)$ spectra in Figure 1. The Eulerian and Lagrangian time scales in βP are then approximately equal because eddies evolve at one point more rapidly than particles are swept through them; the Lagrangian time scale then reflects the short Eulerian scale.

Figure 3 shows y-profiles of Eulerian variance and Reynolds stress for the two inhomogeneous experiments WALL and SHR. In WALL, statistics are reasonably homogeneous except within $y \approx 0.05$ of the wall where v' and ζ' are suppressed and u' is increased; the total kinetic energy varies little across the channel. This behavior is qualitatively similar to that observed in surface currents near the coastal boundary (Davis, 1985). In SHR, u', v' and ζ' are slightly greater where $\partial_y\langle u\rangle$ is greatest but vary little across the sheared flow. The observed mean velocity differs slightly from the true mean ($\langle u\rangle = \sin(2\pi y)$ was imposed) because of sampling error; as seen below the time scale of u' is long in SHR, as it is in βP. In SHR the Reynolds stress $\langle u'v'\rangle$ induced by the imposed mean shear is small and negative and is extreme where $\partial_y\langle u\rangle$ is maximum, consistent with an eddy viscosity notion; the implied momentum diffusivity is about 0.01. The Eulerian time scales in WALL are generally similar to fP, presumably because of the absence of Rossby wave characteristics. The same is true of SHR near $y = 0$ where the Eulerian time scale is not shortened by mean flow advection. The Lagrangian time scales of these flows are discussed further below.
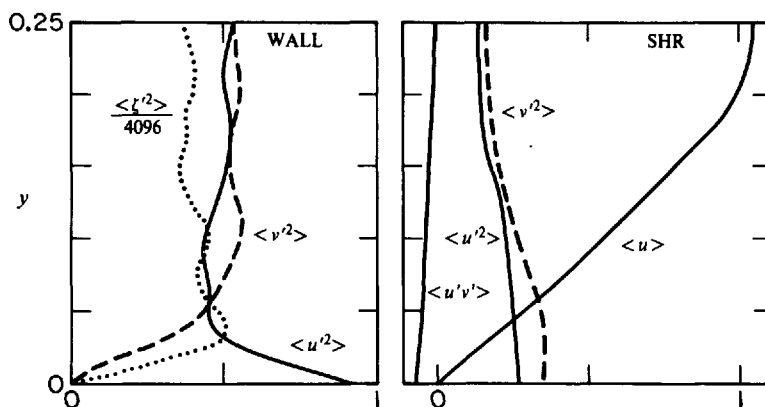

Figure 3. Profiles of Eulerian statistics across the inhomogeneous flows WALL (with $v = 0$ at $y = 0, 0.5$) and SHR (with $\langle u\rangle = \sin 2\pi y$). The shear stress $\langle u'v'\rangle$ is antisymmetric across $y = 0.25$; all other properties are symmetric. In SHR $\langle u\rangle$ is antisymmetric across $y = 0$; all other properties in SHR are symmetric there. At $y = 0$ in SHR $\langle u'v'\rangle \approx -0.01 \, \partial_y\langle u\rangle$.

b. Description of eddy transport. We turn now to examining the magnitude and time variation of the diffusivity $\kappa(\mathbf{x}, t)$ and the characteristic time τ at which reaches its asymptotic value $\kappa^\infty(\mathbf{x})$. Figures 4–6 show the time variation of κ in the various experiments. $\kappa(\mathbf{x}, t - \tilde{t})$ was computed by sampling trajectories periodically to define $\mathbf{x}$ and t and then looking backward through the trajectory to compute $s(\tilde{t}|\mathbf{x}, t)$ of (4.1) at various $\tilde{t}$. Estimates of the time when κ becomes time independent to within sampling error provides the values of τ. Table 2 summarizes κ^∞ and τ for the experiments; the other entries in Table 2 are discussed below.

Figure 4 describes the homogeneous experiments fP and βP; experiment fP is also isotropic so $\kappa_{nm(t)} = \delta_{nm}\kappa(t)$. Figure 5 describes WALL; results are shown for two regions. In the interior region $0.06 < y < 0.25$ both Eulerian and Lagrangian statistics vary slowly with y. Within a boundary layer with thickness of $O(0.05)$ statistics vary rapidly (see also Fig. 3) and the $0 < y < 0.03$ average in Figure 5 is representative of this boundary layer. Figure 6 describes the SHR experiment, again for two regions; $0.19 < y < 0.25$ is typical of the low shear portion of the flow (where the gradient of mean vorticity is greatest) and $0 < y < 0.06$ is a region of large shear. For the WALL and SHR experiments symmetries have been used to collapse all observations into the range $0 < y < 0.25$.

According to (2.5), $\kappa = D \cdot \alpha$ so that α is a characteristic time relating κ and the mean square turbulent velocity. From the summary in Table 2 it is clear that this time is of the same order of magnitude as the time scale computed from rms vorticity or the
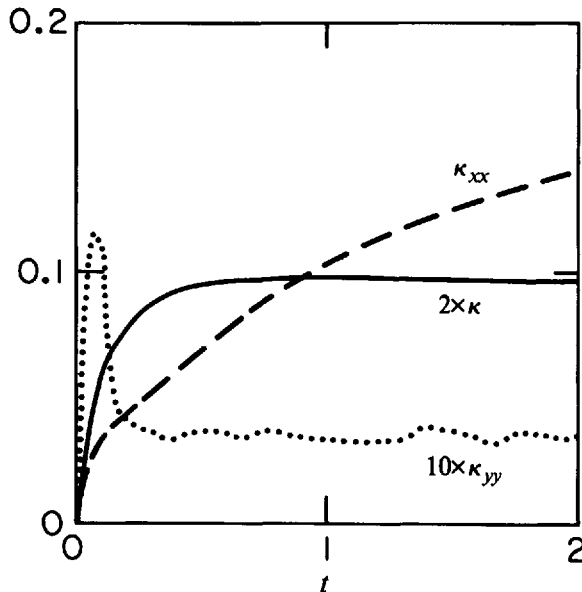

Figure 4. The isotropic diffusivity $\kappa(t)$ for fP (solid) and $\kappa_{xx}(t)$ (dashed) and $\kappa_{yy}(t)$ (dotted) for βP. Note that the values plotted are $\kappa \times 2$ for fP and $\kappa_{yy} \times 10$ for βP.
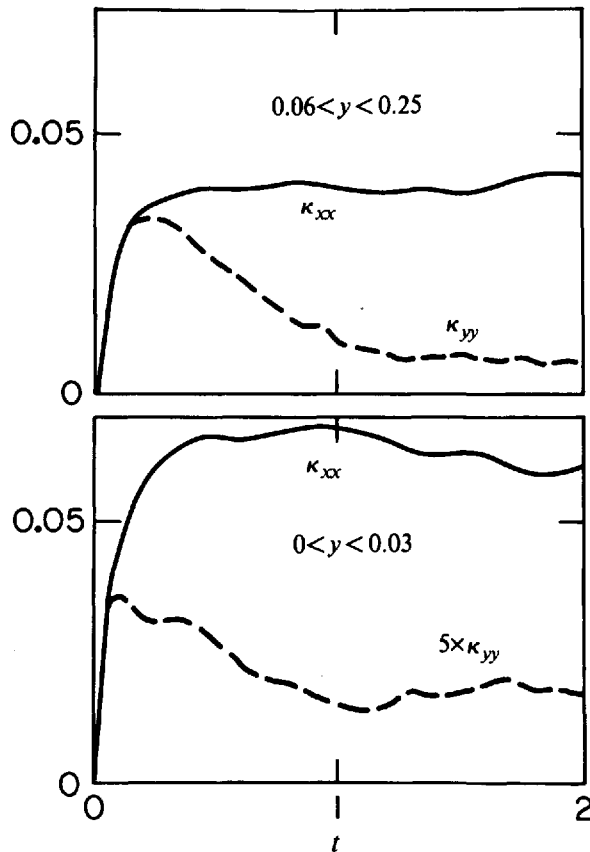
Figure 5. The eddy diffusivities $\kappa_{xx}(y, t)$ (solid line) and $\kappa_{yy}(y, t)$ (dashed line) for WALL in which $v_y = 0$ at $y = 0$ and 0.5. The upper panel corresponds to the relatively homogeneous region away from the walls. Note that κ_{yy} varies on two time scales. The lower panel is the average of $\kappa(y, t)$ over $0 < y < 0.03$, the inner half of the wall boundary layer. By symmetry κ_{yx} and κ_{xy} vanish; κ_{yy} vanishes at $y = 0$.

characteristic velocity and length scales. No simple scaling is, however, capable of describing the variations between experiments and, in contrast to the observation of Price (1983), this characteristic time is certainly not constant. By the same measure, the characteristic length scale κ/u' also shows no evident predictable pattern.

In contrast to the similarity of Eulerian statistics between experiments seen in Figures 1 and 2, the diffusivities differ by nearly two orders of magnitude between experiments. The large β in βP reduces κ_{yy} by a factor of 10 from fP while the zonal diffusivity κ_{xx} is increased by a factor of 3. In the interior region of WALL, κ_{xx} is little changed from fP but κ_{yy} is substantially reduced, showing an unexpected effect of the relatively distant $v = 0$ boundary condition; the Eulerian statistics of Figure 3 give no
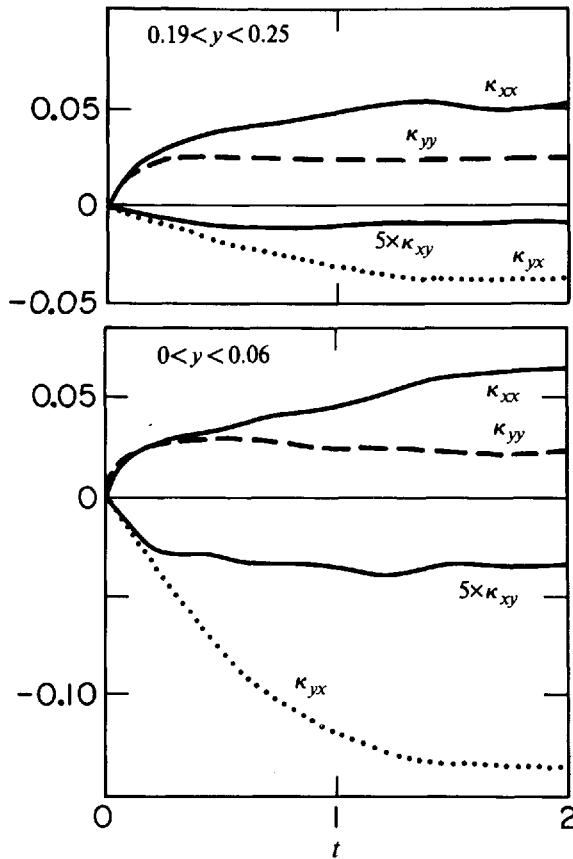
Figure 6. The eddy diffusivities for SHR with $U = \sin (2\pi y)$. The curves are $\kappa_{xx}(y, t)$ (solid), $\kappa_{yy}(y, t)$ (dashed), $\kappa_{xy} - \langle u'_y d_x \rangle$ (dotted) and $\kappa_{yx} - \langle u'_y d_y \rangle$ (solid). Results from $0 < y < 1$ are collapsed into the range $0 < y < 0.25$ using the symmetries about $y - n/4$. The upper panel corresponds to the 25% of the y range with the smallest mean shear, the lower panel to the 25% with the largest shear.

indication of this anisotropy. Within the WALL boundary layer κ_{yy} is much reduced (it must vanish at $y = 0$) while κ_{xx} is increased somewhat. In both regions of SHR the potential vorticity gradient $\partial^2_{yy} U$ produces an effect similar to that of β in βP: κ_{yy} is reduced and κ_{xx} is somewhat increased. The mean shear also generates off-diagonal diffusivity components $\kappa_{yx} - \langle v' s_x \rangle$ and $\kappa_{xy} = \langle u' s_y \rangle$ which are largest where the shear is large. κ is very unsymmetric with $|\kappa_{yx}|$ much exceeding $|\kappa_{xy}|$.

Between experiments the time behavior of the diffusivity κ varies as much as its magnitude but some general comments apply. First, in most cases the time lag τ before κ becomes independent of time is of the order unity, substantially longer than the time scale computed from rms vorticity or from characteristic eddy velocity and space

Table 2. Parameters determining passive scalar transport. Results for WALL and SHR are given for two y ranges. κ^∞ is the asymptotic diffusivity $\kappa(y, \tau)$ where τ is the time beyond which κ does not vary. $\mathfrak{s}^\infty$ is the RMS size of the predictable displacement $\mathfrak{s}$ for time lags greater than τ. In some experiments $\mathfrak{s}_y$ exceeded $\mathfrak{s}_y^\infty$ before equilibrating; the temporary maximum is $\mathfrak{s}_y^{MAX}$. χ is the RMS value of $\chi_r - \chi(\tau | x, t)$, the unpredictable displacement which enters (2.11). In χ_y of WALL $0 < y < 0.03$ and χ_x of SHR $0.19 < y < 0.25$ the mean of χ is a significant part of this RMS value.

Exp.	fP	βP	WALL		SHR	
y			0.06–0.25	0–0.03	0.19–0.25	0–0.06
κ_{xx}^∞	0.05	≈0.2	0.04	0.07	0.05	0.06
κ_{yy}^∞	0.05	0.003	0.01	0.004	0.02	0.02
κ_{xy}^∞			0	0	−0.002	−0.007
κ_{yx}^∞			0	0	−0.04	−0.14
τ	0.3	≈3	1.5	0.3	1.5	1.5
$\mathfrak{s}_x^\infty$	0.07	0.4	0.06	0.07	0.15	0.25
$\mathfrak{s}_y^\infty$	0.07	0.005	0.015	0.01	0.05	0.03
$\mathfrak{s}_y^{MAX}$	0.07	0.02	0.05	0.02	0.06	0.05
χ_x	0.13	0.7	0.4	0.2	1.0	0.7
χ_y	0.13	0.1	0.25	0.2	0.2	0.2

scales; apparently τ is determined by the scales of the largest eddies. Second, variation of κ frequently occurs on two time scales. For example in βP, κ_{yy} equilibrates quickly while κ_{xx} is still varying at the longest observed time lag; in WALL κ_{yy} itself varies on two time scales.

In fP κ equilibrates at $\tau \approx 0.3$. The small β-Rossby number in βP significantly speeds equilibration of κ_{yy} but τ is set by the slow equilibration of κ_{xx} and is too long to be well determined. As was true of the magnitude of κ, the effect of $\partial_{yy}^2 U$ in SHR is similar to that of β in βP: κ_{yy} equilibrates quickly but κ_{xx} requires a long time to reach its asymptote. The slow equilibration of κ_{xx} means that the history corrections to a flux *vs.* gradient law in (2.10) will be relatively important in zonal transport of passive scalars. In WALL κ_{xx} equilibrates quickly but κ_{yy} continues to vary on a time scale of $O(1)$, even in the interior; by comparison with fP, this is another indication of the effect of the distant wall boundary conditions.

The y-variation and sign of the off-diagonal elements of κ in SHR are consistent with mixing length reasoning. For example, at $y = 0$ where $U = 0$ and $\partial_y U$ is largest, particles arriving at $y = 0$ with $v > 0$ have a negative s_x', as if they had adopted the mean velocity for $y < 0$. Similarly, particles which have undergone a positive y displacement arrive with negative u', again appropriate to the mean flow in their previous location. The magnitude of the diffusivity κ_{yy} in SHR is, on the other hand, inconsistent with the notion that either momentum or vorticity is transported like a passive scalar. At $y = 0$ Figure 3 indicates that $-\langle u'v' \rangle \approx 0.07$ and $\partial_y U = 2\pi$; the associated eddy viscosity is only half of κ_{yy}^∞. If ζ were transported like a passive scalar

one would expect

$$- \langle v'\zeta' \rangle = \partial_y \langle v'u' \rangle = -\kappa_{yy}^\infty \partial_{yy}^2 U.$$

Figure 3 shows that $\partial_y \langle v'u' \rangle \approx 0.3$ at $y = \frac{1}{4}$; this corresponds to a vorticity diffusivity of 0.01, again only half of the observed κ_{yy}^∞. One may speculate that the mean vorticity gradient $\partial_{yy} U$ serves to selectively constrain the y-displacement of particles on which vorticity is conserved in the absence of dissipation, much in the manner that β constrains particles in the βP experiment.

In general, these results show that the diffusivity κ and its time variation are strong functions of flow parameters and that their dependence on these parameters is not straightforward. Parameterization of κ, or even κ^∞ will not be easy.

c. Restrictions on validity of the transport model. The conditions under which the elaborated advection-diffusion model (2.10) is valid are given in (2.11) and (2.12). The "scale separation" development of Section 2c is valid if both conditions in (2.11) are met. The "quasi-Gaussian u'" development requires both conditions (2.12) to be met. The scale separation derivation requires particle displacements over time τ to be smaller than L^Θ, essentially the scale of Θ, and smaller than L^x, the inhomogeneity scale of particle displacement statistics. The only scale restriction for the quasi-Gaussian derivation is that the predictable displacement $\tilde{s}$ be smaller than L^x.

Table 2 lists the characteristic displacements which enter into the restrictions (2.11) and (2.12). The values of $\tilde{s}$ listed are standard deviations computed from observed κ's according to (2.5g). Since κ_{yy} sometimes goes through a temporary maximum before reaching its asymptotic limit at time τ, both asymptotic values of $\langle \tilde{s}^2 \rangle^{1/2}$ and maximum values are given. Also listed are typical values of the unpredictable displacement χ_τ over the time lag τ which enters (2.11). These are root-mean-square values computed from the observed mean square of the total displacement $s(t - \tau|\mathbf{x}, t)$ and the variance of $\tilde{s}$.

In all but two cases, the RMS χ values are essentially standard deviations because the mean displacements are negligible. In the WALL boundary layer there is a mean drift of particles toward the wall and this contributes significantly to $\langle \chi^2 \rangle$. Note that $s(t - \tau|\mathbf{x}, t)$ is the displacement before arriving at $\mathbf{x}$; the mean displacement of particles deployed at $\mathbf{x}$ is away from the wall. In SHR $0.16 < y < 0.25$, near the maximum of U, the mean particle velocity is less than U but still large enough to contribute significantly to $\langle \chi_x^2 \rangle$. The mean particle velocity is less than U because most particles arriving at a point in the y range have spent part of their recent history in regions of smaller U.

In all cases the unpredictable displacement $\tilde{s}$ is much smaller than the unpredictable displacement χ_τ. Consequently, meeting requirement $\langle \chi_\tau^2 \rangle^{1/2} \ll L^x$ of (2.11b) will insure meeting $\langle \tilde{s}^2 \rangle^{1/2} \ll L^\Theta + \langle \chi_\tau^2 \rangle^{1/2}$ of (2.11a) so long as L^Θ is not much smaller than L^x. At the same time, the requirement $\langle \chi_\tau^2 \rangle^{1/2} \ll L^x$ of the scale separation development
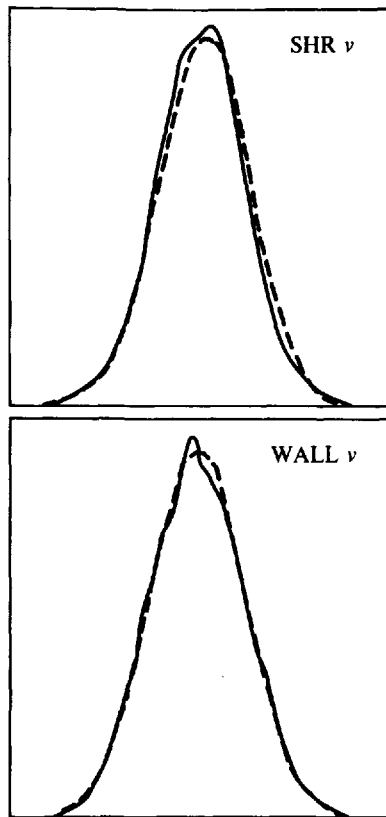
Figure 7. Examples of sample histograms of turbulent velocity (solid) (dashed) compared with Gaussian probability densities computed from the sample mean and variance. The upper panel is v' from $0.19 < y < 0.25$ of SHR. The lower panel is v' from $0.12 < y < 0.25$ of WALL. These examples were selected as the poorest comparisons with Gaussian distributions and are therefore worst case tests of restriction (2.12a).

is much more stringent than the restriction $\langle \tilde{s}^2 \rangle^{1/2} \ll L^x$ placed on the quasi-Gaussian u' derivation.

Figure 7 shows two examples of sample histograms of u' from which the quasi-Gaussian u' requirement can be evaluated. These examples were selected from the many histograms computed for various experiments as showing the largest departures from a Gaussian distribution. The departures are still small and the normalized higher cumulants are negligible within sampling error. At least in these experiments, the probability density functions of turbulent velocity fluctuations are sufficiently close to normal distributions to meet requirement (2.12a).

In the homogeneous experiments f P and βP the conditions on L^x are automatically satisfied and the velocity histograms are even closer to Gaussian than those shown in Figure 7. Thus the quasi-Gaussian derivation should be valid. The scale separation

development is valid in fP so long as $L^Q \gg 0.007$, which is not very restrictive. Validity of this development for βP rests on $L^Q_y \gg 0.005$ and $L^Q_x \gg 0.7$; the latter of these is fairly stringent. Validity of the scale separation derivation is, however, academic since the quasi-Gaussian $\mathbf{u}'$ development is valid.

In the interior of the WALL flow, spatial derivatives of particle statistics are difficult to detect so L^x is at least $O(1)$. This is much larger than $\tilde{s}^{MAX}_y = 0.05$ which, coupled with a closely Gaussian distribution of $\mathbf{u}'$, means that the quasi-Gaussian $\mathbf{u}'$ model is valid. L^x is also somewhat larger than the y component of $\chi_r = 0.25$, so the scale separation derivation may be valid so long as L^Q_x is much larger than 0.4, which is again quite stringent.

In the WALL boundary layer $L^x_y = O(0.05)$. This is substantially larger than the asymptotic $\tilde{s}^y$ and of the same order as its maximum; as long as the effects of the transient maximum are not serious the quasi-Guassian $\mathbf{u}'$ model should be acceptable. On the other hand, the y component of χ_r is much larger than L^x_y and the scale separation derivation is invalid.

The inhomogeneity scale in SHR is $L^x_y = \frac{1}{2}\pi$. Again this is not smaller than the y component of χ_r so the scale separation derivation of (2.10) is invalid. On the other hand, $\mathbf{u}'$ is reasonably Gaussian and $\tilde{s}_y = 0.05$ at least marginally meets (2.12b) so that the quasi-Gaussian $\mathbf{u}'$ model should be reasonably accurate.

d. Conclusions. Analysis of particle motion in simulated geophysical turbulence leads to three conclusions. First, the variations of single-particle diffusivity between different flow regimes are large and difficult to predict from simple scaling arguments. Second, derivations of diffusive flux laws from scale separation assumptions alone appear applicable only to a restrictive class of flows. Third, the requirements of the quasi-Gaussian $\mathbf{u}'$ derivation of the elaborated advection-diffusion model (2.10) seem to be met for a broad range of flows.

I have been unable to rationalize the large variations of κ in the experiments described above using any simple scaling laws. It must be expected that dynamicists will continue to use such scale arguments to measure the importance of eddy fluxes relative to advection, but I believe such estimates will generally be in error by an order of magnitude or two. One must even be cautious about the applicability of numerical simulations for determining κ. For example, the suppression of κ_{yy} by β in βP presumably occurs because particles cannot change their y position much without accumulating unacceptable relative vorticity. Thus to provide accurate particle motion statistics models must, firstly, conserve vorticity along trajectories very much as the ocean does and, secondly, allow accurate determination of the trajectories along which vorticity is so conserved. In limited resolution models employing artificial enstrophy absorbing viscosities (such as the model employed here) it is unclear how well this can be done.

It is perhaps surprising that scale separation derivation of the advection-diffusion model has such limited validity. This is particularly so because the restrictions on the

development of Section 2c, which uses the statistical trajectory prediction model, are much less severe than those placed on the conventional heuristic development (*cf.* the Appendix). Nevertheless, the requirements on the scale separation development are not met in many inhomogeneous flows and place severe restrictions on the scale of Θ in some homogeneous flows.

Fortunately, mean transport can be modelled without resolving all scales of motion when the requirements of the quasi-Gaussian $\mathbf{u}'$ model are met, and they are met in all cases studied here. This is, of course, not a demonstration that all geophysical turbulence produces Gaussian $\mathbf{u}'$ fluctuations. The flows examined here are relatively heavily damped and forced by Gaussian random torques; this may not be representative of oceanic mesoscale turbulence. Clearly the kind of submesoscale coherent vorticies discussed by McWilliams (1985) are not Gaussian perturbations in detail; they may represent small perturbations to the distribution of velocity but certainly not to vorticity. It is important to note, with regard to this model, that the requirement of quasi-Gaussian $\mathbf{u}'$ is much less severe than the assumptions used to develop quasi-Gaussian closures of the full momentum or scalar transport equations. In the latter, the *joint probability densities of* $\mathbf{u}'$ *and* θ, *or* $\mathbf{u}'$ *at two or more locations, are related to* joint-normal distributions. Here only the probability density of $\mathbf{u}'$ at a single location need have an approximately Gaussian shape.

4. Conclusions

The principal results of this paper are the derivations of the mean transport equation

$$\partial_t \Theta(\mathbf{x}, t) + \mathbf{U}(\mathbf{x}) \cdot \nabla \Theta(\mathbf{x}, t) - Q(\mathbf{x}, t)$$

$$= \nabla \cdot \kappa(\mathbf{x}, t) \cdot \nabla \Theta(\mathbf{x}, t) + \nabla \cdot \int_0^t d\tilde{t} \frac{\partial \kappa(\mathbf{x}, t - \tilde{t})}{\partial \tilde{t}} \cdot \nabla \{\Theta(\mathbf{x}, t) - \Theta(\mathbf{x}, \tilde{t})\}$$

$$- \nabla \cdot \int_0^t d\tilde{t} \frac{\partial \kappa(x, \tilde{t})}{\partial \tilde{t}} \nabla \Theta(\mathbf{x}, t - \tilde{t}) \quad (4.1)$$

for passive Θ-stuff and the examination of the validity of the derivations in simulated geophysical turbulence. The requirements for the quasi-Gaussian $\mathbf{u}'$ development were met in all cases tested but the derivation based solely on scale separation arguments was valid only in essentially homogeneous flows. The diffusivity in (4.1) is an observable transport parameter (as opposed to a phenomenological one) which is a function of position and time lag:

$$\kappa_{nm}(\mathbf{x}, t) = \langle u_n'(\mathbf{x}, 0)\{r_m(0|\mathbf{x}, 0) - r_m(-t|\mathbf{x}, 0)\} \rangle. \quad (4.2)$$

This mixed Eulerian-Lagrangian statistic is the covariance of the velocity deviation from the Eulerian mean at $\mathbf{x}$ and the displacement over time lag t that particles undergo at arriving at $\mathbf{x}$.

From the theoretical perspective these results have several implications. Perhaps most important is the conclusion that the concept of eddy diffusion can be rationalized with physically simple and testable approximations of particle trajectory statistics without introducing phenomenological parameters. Although not the first development of an eddy diffusion model, I believe the present one is logically straightforward and yet involves only requirements which are widely applicable. The derivations are unique in starting with the exact formal solution of the Lagrangian form of the transport equations. The average of this solution is then simplified using a statistically optimized model predicting a particle's trajectory from a few observable variables (position and a single velocity). One might hope that this approach can be applied to other, more difficult, transport problems such as the eddy fluxes of dynamically active quantities like density and potential vorticity.

Recent theoretical work by Rhines and Young (1982) and by Luyten *et al.* (1983) have emphasized the importance of lateral transport of potential vorticity and the relative strength of its advective and eddy fluxes. Unfortunately, the present study does not address the question of how well eddy transport of potential vorticity can be modelled as diffusion. Rhines and Holland (1979) outline an approach toward such modelling and present examples of its consequences for ocean circulation. It would seem of the highest priority to extend this approach to a tested model of eddy transport of dynamically active tracers in general, and potential vorticity in particular.

The eddy transport model (4.1) is not a pure advection-diffusion equation. The eddy flux law (2.7) upon which it is based includes an effect of the recent history of the Θ gradient. This is a consequence of the finite scale of the dispersing eddies and represents the difference between dispersion by molecules, with their essentially infinitesimal scales, and by eddies. In the present model the driving potential for the eddy flux at time t is the sum of prior mean field gradients at time $t - \tilde{t}$ weighted by the time change of the diffusivity κ at time lag $\tilde{t}$. If time variations of κ are limited to a time range less than τ then only the history of $\nabla\Theta$ over $t - \tau < \tilde{t} < t$ affects the flux at time t. If τ is small compared with the characteristic time over which Θ varies then a pure eddy diffusion model with the large time asymptotic diffusivity κ^∞ obtains.

Because of the long use of models based on pure eddy diffusion, it is important to define the influence of this history correction in the evolution of Θ fields. A pure advection-diffusion equation naturally introduces a single dimensionless scaling parameter, the Peclet number $Pe = U_c L_c / \kappa$, where U_c and L_c are a characteristic velocity and length. Pe measures the relative importance of advection and diffusion. The history correction in (4.1) depends on the history over the interval τ, the time over which the diffusivity approaches its asymptote, and this introduces a second parameter $Hi = \tau / T_c$ where T_c is the time scale on which Θ varies. Hi measures the relative importance of the history correction in the total eddy flux. In the limit $Hi \rightarrow 0$ the effect of finite eddy scales vanishes and a pure advection-diffusion equation is recovered. Specifically, in a steady state (4.1) reduces to pure advection-diffusion.

The history correction is particularly simple when variation of κ takes the form

$$\kappa(\mathbf{x}, t) = \kappa^{\infty}(\mathbf{x})[1 - \exp(-t/\tau)].$$

In this case, straightforward manipulation of (4.1) yields

$$\left[\tau \frac{\partial}{\partial t} + 1\right]\left[\frac{\partial}{\partial t}\Theta + \mathbf{U} \cdot \nabla\Theta - Q\right] = \nabla \cdot \kappa^{\infty} \cdot \nabla\Theta. \qquad (4.3)$$

The effect of finite eddy scales, and the consequent time variations of κ, is to raise the order of the transport equation in t. The additional initial condition

$$\frac{\partial}{\partial t}\Theta = 0 \quad \text{at } t = 0$$

follows directly from (4.1).

The effect of the history correction is easy to see in a one-dimensional zero-source constant-diffusivity initial value problem when (4.3) is easily solved by decomposing Θ into Fourier components of the form $a(k, t) \exp(iky)$. Figure 8 presents the evolution of Θ from the initial condition $\Theta(\mathbf{x}, 0) = \exp(-y^2/2L_c)$ for two values of $\kappa^{\infty}\tau/L_c^2$. The character of evolution depends strongly on this parameter because Fourier components with $k^2 \ll \tau/\kappa^{\infty}$ behave quite differently from those with $k^2 \gg \tau/\kappa^{\infty}$.
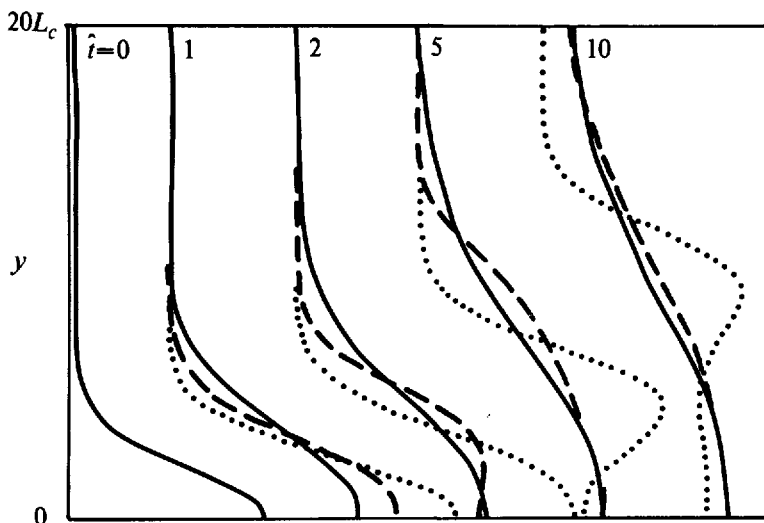

Figure 8. Profiles of $\Theta(y, t)$ for the elaborated diffusion equation (4.2) for different equilibration times τ. Curves are Θ *vs.* y at various values of $\hat{t} = t\kappa^{\infty}/L_c^2$ where L_c is the scale of the initial Gaussian disturbance. For graphical clarity profiles are normalized by $(L_c^2 + 2\kappa^{\infty}t)^{1/2}$. The curves correspond to $\kappa^{\infty}\tau/L_c^2 = 0.1$ (solid), 1.0 (dashed) and 4.0 (dotted). The curve for the smallest τ is indistinguishable from pure diffusion. For larger τ the effect of the finite propagation speed $C = (\kappa^{\infty}/\tau)^{1/2}$ is evident.

For small k the basic Θ time scale is $1/k^2\kappa^\infty$, just as in a pure diffusion problem. In this case the extra time derivative in (4.3) is important only during an initial transient during which Θ changes little. For $\kappa^\infty\tau/L_c^2 \ll 1$ the initial field is composed entirely of components with $k^2 \ll \tau/\kappa^\infty$ and evolution of Θ is essentially as it is in pure diffusion.

For $k^2 \gg \tau/\kappa^\infty$ a Fourier component evolves as

$$a(k, 0) \exp -\frac{t}{2\tau} + ik(y - Ct) \quad \text{where } C = (\kappa^\infty/\tau)^{1/2},$$

that is as a damped nondispersive wave. This behavior is quite different from a pure diffusion equation as the solution for large $\kappa^\infty\tau/L_c^2$ in Figure 8 shows. It is interesting that in (4.3), unlike a pure diffusion model, the disturbance from an initial delta function does not propagate with infinite speed but rather at the speed $(\kappa^\infty/\tau)^{1/2}$ which is of the same order as the eddy velocities; this finite propagation speed effect is evident in Figure 8.
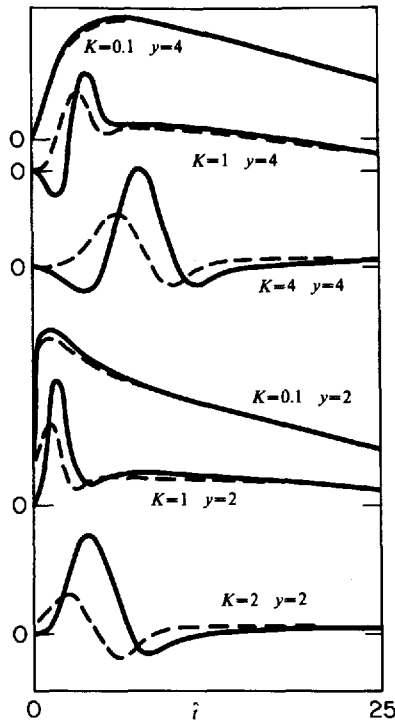

Figure 9. The instantaneous mean eddy flux of Θ-stuff (solid) and $-\kappa^\infty\partial_y\Theta$ (dashed) for the elaborated diffusion equation (4.2). The upper three time series are values at $y = 4$ and the lower three are at $y = 2$. The time axis is $\hat{t} = t\kappa^\infty/L_c^2$ where L_c is the initial Gaussian disturbance's scale. At each y curves are shown for three values of $K = \kappa^\infty\tau/L_c^2$. For graphical purposes each curve has been multiplied by $L_c^2 + 2\kappa^\infty t$. Note that only for small K or large $\hat{t}$ do the instantaneous flux and the scaled gradient coincide.

Available results for lateral dispersion in the ocean (*cf.* Freeland *et al.* (1975) and Price (1983)) indicate $\kappa^\infty = O(10^3 \text{ m}^2/\text{s})$ and $\tau = O(10 \text{ days})$. Although these sizes, largely based on assuming low frequency variations result from the mean flow, may underestimate κ^∞ and τ, they indicate that mean lateral dispersion of features with $L_c >$ 30 km is well modelled by pure advection-diffusion. Only for fields in which time changes following a mean particle path occur on time scales of the order 10 days would the history correction to pure advection-diffusion be important.

From the observational perspective the results here have additional implications. Because the diffusivity in the transport model is defined in terms of statistics of particle trajectories it is, in principle, observable. At least for lateral transport it is possible that the transport parameters U, κ and τ can be determined from the statistics of pseudo-Lagrangian drifter and float trajectories. To do this it is first necessary to demonstrate that the differences between floats and ideal continuum flow particles are small enough that particle and float statistics are similar. It is not, however, necessary that floats follow ideal particles on a realization by realization basis; only statistical similarity is required. Secondly, it is necessary that repeated observations be taken in the same locality so that the mean flow can accurately be determined. To infer mean flow from the low frequency component of a single float's velocity is to assert, rather than determine, that low frequency eddy motion is not important to eddy transport. It is also important that float trajectory analyses determine the time scale τ over which the diffusivity approaches its asymptotic value.

Finally it must be noted that, to the extent that the eddy flux depends on the history of the mean field gradient, the diffusivity can not be determined from the ratio of the eddy flux and the instantaneous mean gradient. Figure 9 presents time series of the gradient $\partial_y \Theta$ and the eddy flux for the examples shown in Figure 8. Clearly, when $\kappa^\infty \tau / L_c^2$ is not small there are large fluctuations in the ratio of instantaneous flux and mean gradient.

APPENDIX

The heuristic advection-diffusion model

The use of an advection-diffusion model for mean transport is frequently justified by a heuristic analogy to molecular transport with the justification that eddy time and space scales are small compared with the scales of the mean velocity and concentration fields. The purpose of this Appendix is to show how conventional scale separation arguments reduce (2.2) to an advection-diffusion model but that the range of validity is much more restrictive than for the transport models of Section 2.

a. Development. The crucial step in the conventional development of an advection-

diffusion model for Θ is the assumption that transport is, over some time step Δ, a Markov process in the sense that particle motion over that time step depends statistically only on particle positions at its start. If a particle's motion for $t > t_1 + \Delta$ is statistically independent of its history before time t_1 then the history integral in (2.2) can be broken into time steps of Δ and an evolution equation developed. More precisely, if the transition probability of a particle going from $\tilde{\mathbf{x}}$ at $\tilde{t}$ to $\mathbf{x}_1$ at $\tilde{t} + \Delta$ to $\mathbf{x}$ at t is the product of the probabilities for the individual transitions then

$$C(\mathbf{x}, t + \Delta - \tilde{t}, \tilde{\mathbf{x}}) = \int d\mathbf{x}_1 \, C(\mathbf{x}, \Delta, \mathbf{x}_1) \cdot C(\mathbf{x}_1, t - \tilde{t}, \tilde{\mathbf{x}}). \qquad (A.1)$$

From (A.1) one can construct $C(\mathbf{x}, n\Delta, \tilde{\mathbf{x}})$ as the n-fold convolution of $C(\mathbf{x}, \Delta, \tilde{\mathbf{x}})$. This leads directly to the local-in-time evolution equation

$$\Theta(\mathbf{x}, t + \Delta) = \int d\tilde{\mathbf{x}} \, C(\mathbf{x}, \Delta, \tilde{\mathbf{x}}) \Theta(\tilde{\mathbf{x}}, t) + \Delta \overline{Q}(\mathbf{x}, t) \qquad (A.2)$$

where

$$\overline{Q}(\mathbf{x}, t) = \frac{1}{\Delta} \int_t^{t+\Delta} d\tilde{t} \int d\tilde{\mathbf{x}} \, C(\mathbf{x}, t - \tilde{t}, \mathbf{x}) Q(\tilde{\mathbf{x}}, \tilde{t}). \qquad (A.3)$$

If the scales of Θ and Q are large compared to particle displacements over the interval Δ, a Taylor series expansion of $\Theta(\tilde{\mathbf{x}})$ and $Q(\tilde{\mathbf{x}})$ about $\tilde{\mathbf{x}} = \tilde{\mathbf{x}}$ in (A.2) and (A.3) yields the local-in-space model

$$\frac{\Theta(\mathbf{x}, t + \Delta) - \Theta(\mathbf{x}, t)}{\Delta} + V_n \frac{\partial}{\partial x_n} \Theta(\mathbf{x}, t)$$

$$- \frac{\partial}{\partial x_n} \nu_{nm}(\mathbf{x}, \Delta) \frac{\partial}{\partial x_m} \Theta(\mathbf{x}, t) + \frac{1}{\Delta} \int_t^{t+\Delta} d\tilde{t} \, Q(\mathbf{x}, \tilde{t}), \quad (A.4)$$

where

$$\mathbf{s}(\Delta | \mathbf{x}) = \mathbf{x} - \mathbf{r}(-\Delta | \mathbf{x}, 0)$$

is the displacement from time $-\Delta$ to time 0 that a particle undergoes in arriving at $\mathbf{x}$,

$$\nu_{nm}(\mathbf{x}, \Delta) = \frac{\langle s_n(\Delta | \mathbf{x}) s_m(\Delta | \mathbf{x}) \rangle}{2\Delta}$$

is the apparent diffusivity involving the mean product of particle displacements over interval Δ,

$$\Delta \mathbf{V}(\Delta | \mathbf{x}) = \int d\tilde{\mathbf{x}} (\mathbf{x} - \tilde{\mathbf{x}}) \cdot C(\tilde{\mathbf{x}}, \Delta, \mathbf{x}) = \langle \mathbf{s}(\Delta | \mathbf{x}) \rangle$$

is the mean displacement over the interval Δ of those particles arriving at $\mathbf{x}$, and

$$\tilde{V}_n(\Delta | \mathbf{x}) = V_n(\Delta | \mathbf{x}) + \frac{\partial}{\partial x_m} \nu_{mn}(\mathbf{x}, \Delta)$$

is the advection velocity. Clearly (A.4) is a finite time-step analog of the advection-diffusion model.

There are two interesting points about the advection velocity $\tilde{V}$. First, the mean particle velocity V differs from the advection velocity $\tilde{V}$ by a bias which is directed away from regions of high diffusivity. This is opposite to the mean drift toward high diffusivity of particles released at a point. The difference arises because we are here interested in the displacement **s** particles undergo in arriving at a point and (*cf.* Davis, 1983) this displacement is biased away from high ν just as displacements from that point are biased toward high ν. Secondly, in the absence of ν variation the advection velocity in (A.4) is the Lagrangian mean velocity V not the Eulerian mean velocity $U = \langle \mathbf{u} \rangle$ normally appearing in advection-diffusion models; when the velocity field $\mathbf{u}$ is nondivergent, as considered here, this difference vanishes.

b. Discussion. The development above parallels that followed for other Fokker-Planck equations (*cf.* Chandrasekhar, 1943) except that the time step Δ is necessarily finite. The principal elements leading to the advection-diffusion model are the assertion of a Markov evolution over the time interval Δ (hence Δ must be large) and the Taylor series expansion of Θ in powers of **s**, the displacement over that time. The minimum size of Δ (and hence of the displacement **s** over that time) for which the Markov assumption is valid is critical to the accuracy of the spatial Taylor series by which (A.2) and (A.3) are converted to the spatially local (A.4).

What determines the minimum useable Δ? We know from the work of Taylor (1921) that when V vanishes and the flow is statistically stationary in **x** and t then the single particle diffusivity is

$$\kappa_{nm}(t) = \frac{1}{2} \frac{d}{dt} \langle s_n(t) s_m(t) \rangle = \frac{1}{2} \int_0^t d\tilde{t} [L_{nm}(\tilde{t}) + L_{mn}(\tilde{t})]$$

where

$$L_{nm}(t) = \langle u_n(t_1 | \mathbf{x}, 0) u_m(t_1 + t | \mathbf{x}, 0) \rangle$$

is the Lagrangian covariance of particle velocity. As $t \to \infty$ the diffusivity κ approaches a constant κ^∞ and

$$\langle s_n(t) s_m(t) \rangle = |\kappa_{nm}^\infty| \cdot |t - t_{nm}|$$

where the t_{nm} are constants of the order τ, the time scale of the Lagrangian covariance L.

In this homogeneous and stationary case Δ must be much larger than the time scale τ over which $L(t)$ goes to zero. To see this, we note that the advection-diffusion model predicts the area

$$A(t) = \int d\mathbf{x} |\mathbf{x}|^2 \Theta(\mathbf{x}, t)$$

to vary as

$$A(t + \Delta) - A(t) = \langle s^2(\Delta) \rangle$$

if $\int d\mathbf{x} \, \Theta = 1$. Thus a model employing $\Delta = T/2$ will predict $A(T) = 2 \langle s^2(T/2) \rangle$ whereas $\Delta = T$ will predict $\langle s^2(T) \rangle$. Because $\langle s^2 \rangle$ is not simply proportional to time, the fractional difference between these is $O(\tau/\Delta)$; thus accuracy of the local-in-time models (A.2) and (A.3) require $\Delta \gg \tau$. The requirement $\Delta \gg \tau$ coupled with the restriction that the typical displacement $|\mathbf{s}(\Delta|\mathbf{x})|$ be much smaller than the scales of Q and Θ presents a stringent limitation on the applicability of this development. In particular the requirement is more restrictive than that in the scale separation development of Section 2.c by the order Δ/τ which must be large. The results of Section 3 suggest that, in general, τ is substantially longer than an eddy turnover time.

The conventional scale separation development is even less satisfactory when there is statistical inhomogeneity and mean shear. The minimum Δ is more difficult to determine when the flow is statistically inhomogeneous because particle velocity statistics are generally not stationary and the arguments above do not pertain; it can only be conjectured that a Δ much greater than the velocity decorrelation scale will be adequate. Further, the requirement that displacements be small compared with the scales of Q and Θ is much more stringent when there is a mean shear because the displacement $\mathbf{s}$ includes displacement by the mean flow and its mean square, therefore, grows more rapidly.

REFERENCES

Bendat, J. S. and A. G. Piersol. 1971. Random Data: Analysis and Measurement Procedures, Wiley-Interscience, NY, 407 pp.

Chandrasekhar, S. 1943. Stochastic problems in physics and astronomy. Rev. Modern Physics., *15*, 1–89.

Csanady, G. T. 1973. Turbulent Diffusion in the Environment, §2.9, D. Reidel, Boston. 248 pp.

Davis, R. E. 1982. On relating Eulerian and Lagrangian velocity statistics: single particles in homogeneous flows. J. Fluid. Mech., *114*, 1–26.

—— 1983. Oceanic property transport, Lagrangian particle statistics, and their prediction. J. Mar. Res., *41*, 163–194.

——1985. Drifter observations of coastal surface currents during CODE: The statistical and dynamical views. J. Geophys. Res., *90*, 4756–4772.

Freeland, H. F., P. B. Rhines and H. T. Rossby. 1975. Statistical observations of the trajectories of neutrally buoyant floats in the North Atlantic. J. Mar. Res., *33*, 383–404.

Haidvogel, D. B. and T. Keffer. 1984. Tracer dispersal by mid-ocean eddies. Dyn. Atmos. Oceans, *8*, 1–40.

Holloway, G. and S. S. Kristmannsson. 1984. Stirring and transport of tracer fields by geostrophic turbulence. J. Fluid Mech., *141*, 27–50.

Luyten, J. R., J. Pedlosky and H. Stommel. 1983. The ventilated thermocline. J. Phys. Oceanogr., *13*, 292–309.

McWilliams, J. C. 1985. Submesoscale, coherent vorticies in the ocean. Rev. Geophys., *23*, 165–182.

Price, J. F. 1983. Particle dispersion in the western North Atlantic (unpublished manuscript). Results are given in chapters 4 and 5 of Eddies in Marine Science, A. R. Robinson, ed., Springer-Verlag, Berlin, 609 pp.

Rhines, P. B. and W. R. Holland. 1979. A theoretical discussion of eddy-driven mean flows. Dyn. Atmos. Oceans, *3*, 289–325.

Rhines, P. B. and W. Young. 1982. A theory of wind-driven ocean circulation, I. Mid-ocean gyres. J. Mar. Res., *40*, 559–596.

Taylor, G. I. 1921. Diffusion by continuous movements. Proc. London Math. Soc., *20*, 196–212.